Phase formation and high dielectric constant of calcium copper titanate using sol–gel route

S. Jesurani · S. Kanagesan · R. Velmurugan · T. Kalaivani

Abstract Nano-sized calcium copper titanate (CCTO) powder was synthesized from a quick and innovative sol–gel process. Calcium nitrate, copper nitrate and titanium isopropoxide were used as the raw materials to synthesize the precursor product. The dried precursor powder was then milled and calcined at 450, 550, 650, 800, 850 and 950 °C for 3 h. The XRD results of the powder calcined at 800 °C indicates the formation of CCTO single phase. AFM studies shows that the average particle size of CCTO powder ranges around 80 nm. From the FTIR spectra the modes observed at 606, 525 and 463 cm^{-1} was assigned to vibration modes of Ca–O, Cu–O and Ti–O–Ti, respectively. The samples sintered at 1,040 °C shows high density (96%) as compared to the theoretical value. The grain sizes of sintered pellets were determined by FE-SEM and the dielectric properties were studied by LCR meter.

1 Introduction

$CaCu_3Ti_4O_{12}$ (abbreviated as CCTO) [1, 2] is a novel material with high relative dielectric constant and low loss tangent, CCTO belongs to a family of oxides of the type $ACu_3Ti_4O_{12}$ [3] and was studied nearly 30 years ago. $CaCu_3Ti_4O_{12}$ was first reported by Subramanian et al. [1] to have an unusually high dielectric constant (~10,000) at

1 kHz. Normally, high dielectric constants are found in ferroelectric materials. $CaCu_3Ti_4O_{12}$ was not found to be a ferroelectric material and has therefore been a material which needed more studies. This material exhibits a giant dielectric constant response with highly unusual temperature independence. It has a high and relatively temperature independent low-frequency dielectric constant over a wide temperature range between 100 and 600 K. However, below 100 K its value drops abruptly by almost three orders of magnitude, an effect that is not accompanied by a long-range structural phase transition [1, 2]. Its structure (space group Im3) can be derived from the ideal cubic perovskite structure by superimposing a body centered ordering of Ca and Cu ions and a pronounced tilting of the titanium centered octahedral [4, 5]. Materials with high dielectric constants and low loss tangents are widely used in technological applications such as capacitors, resonators, and filters. High dielectric constants allow miniaturization of components, thus offering the opportunity to decrease the size of electronic devices [6]. CCTO was generally prepared by the conventional solid state method [7–10]. But it suffers from the disadvantages of chemical inhomogeneity leading to coarse particle size for the product. [11]. It is well known that the electrical properties can be considerably improved when the ceramic is of a homogeneous microstructure [12].

Sol–gel method has the advantage of preparing multi component system with high homogeneity. Since the mixing is carried out in solution state, the homogeneity of the system is in the molecular level. Compared with the conventional mechanical milling method for the preparation of raw powders, the sol–gel method yields ultrafine powders with homogeneity in the molecular scale, inducing a fine microstructure of the sintered ceramic [13]. However, despite the many investigations concerned with

S. Jesurani (✉) · S. Kanagesan · R. Velmurugan · T. Kalaivani
Center for Material Science and Nano Devices Department
of Physics, SRM University, Kattankulathur, Tamil Nadu
603203, India
e-mail: jesuphy@gmail.com

S. Jesurani
Department of Physics, Jeyaraj Annapackium College
for Women, Periyakulam, Tamil Nadu 625601, India

CCTO, there were few reports on the sol–gel processing to synthesize CCTO [11, 14]. The relative dielectric constant of the CCTO ceramic prepared by the sol–gel method by Jha et al. [11] was below 4×10^3, which was much smaller than that of CCTO ceramic ($\sim$12,000) prepared by the conventional solid-state method [1]. In this paper, the synthesis of CCTO ceramic by the sol–gel method has been reported. The development of the microstructure of CCTO under different heat treatments has been investigated. The relative dielectric constant and loss tangent of CCTO at room temperature have been found to be $\sim10^4$ and 0.1, respectively, in the frequency range from 50 Hz to 1 MHz.

2 Experimental techniques

The flow chart for the preparation of calcium copper titanate is shown in Fig. 1. The metal nitrates and Titanium tetraisopropoxide ($Ti(OC_3H_7)_4$) were used as the raw materials; glacial acetic acid and citric acid were the chelating reagent. In a typical run, the appropriate amounts of $Ca(NO_3)_2 \cdot 4H_2O$ and $Cu(NO_3)_2 \cdot 3H_2O$ were dissolved in C_2H_5OH to form solution 1. Titanium tetra isoproxide $Ti(OC_3H_7)_4$ stabilized by acetylacetone was dissolved in isopropyl alcohol, to form solution 2. The solution 1 was added into solution 2 and stirred continuously using a magnetic stirrer at room temperature. Finally, acetic acid and citric acid was added into this mixture. The experiment was performed at low temperature. The blue color sol was obtained after stirring and hydrolyzing the mixture solution for 3 h. Then the mixture was concentrated and the viscous liquid began to form a transparent viscous gel. Finally, a
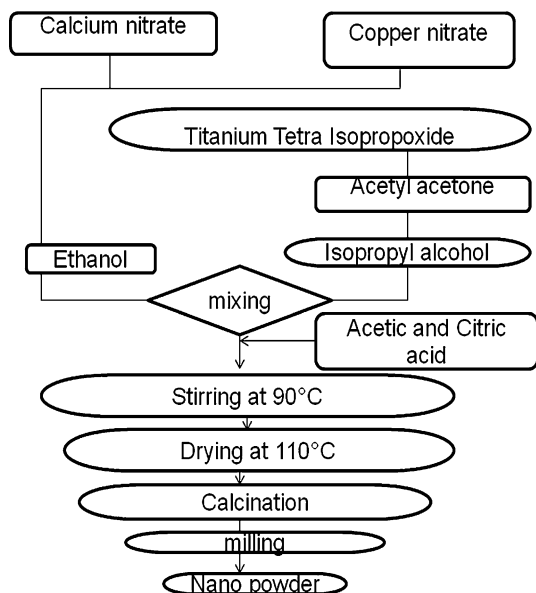
loose and brown ash powder was obtained after the dried gel was being annealed at 110 °C for 2 days. Subsequently, the dried precursor calcined at 450, 550, 650, 800, 850 and 950 °C for 3 h for complete crystallization and then the milling process was carried out in order to get a nano powder. The precursor powder was characterized to identify the phases formed and structural aspects using DTA/TGA, FTIR, XRD morphology using AFM, FE-SEM and dielectric properties using LCR meter etc.

3 Result and discussion

Figure 2 shows the thermal analysis, TG-DTA curves of precursor powder of CCTO from room temperature to 1,200 °C in air with a heating rate of 10 °C per minute. The TG curve showed a weight loss of about 63% in the temperature range from room temperature to 1,200 °C. The weight loss is related to the decomposition and combustion of organic matrix. The DTA curve showed endothermic peak at 159 °C and exothermic reaction at 277 °C, at temperature 159 °C, the weight-loss is 6%. The physically adsorbed water is removed. The residue is gray to black in colour. At temperature, 277 °C the thermal events is associated with the burnout of organic species involved in the precursor powders [15]. The weight loss is 43% in the temperature range from 150 to 550 °C and its may be due to the decomposition of copper nitrate, calcium nitrate and titanium isopropoxide [16–18] and formation of CuO, $CaTiO_3$ which is confirmed by the XRD for samples calcined at 450 and 550 °C. From 550 to 1,200 °C the weight loss is 14%. The XRD pattern shows the formation of homogeneous single phase CCTO at 800 °C. The material starts to melt at 1,080 °C. Julie et al. [7] have reported the synthesis of CCTO, by solid state reaction method using

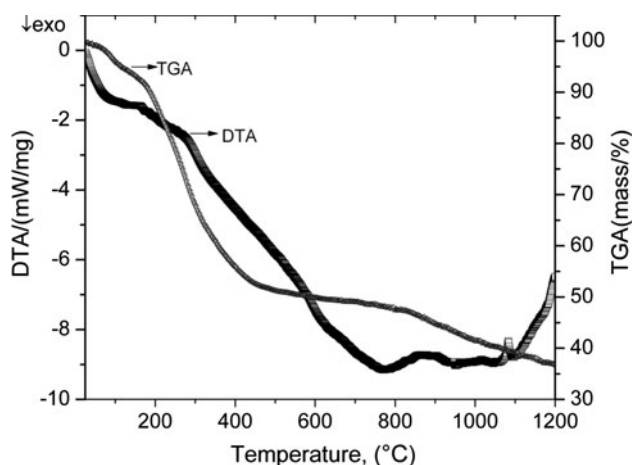Fig. 1 Flow chart for the preparation of calcium copper titanate

Fig. 2 TG-DTA curves of the thermal decomposition of CCTO precursor at a heating rate of 10 °C min^{-1} in static air

$CaCO_3$, TiO_2 and CuO as raw materials, melted at 1,000 °C. Theoretically, the Cu^{2+} cation is reduced at T $\sim$1,000 °C into Cu^+. The Cu^+ will reoxidize during the cooling. Subramanian et al. [1] also reported the existence of impurity CuO in their samples of CCTO. Julie et al. [7] proposed a mechanism that CCTO undergoes a partial phase transition at 1,000 °C, with the formation of Cu_2O phase.

The FTIR spectra of CCTO powder calcined at different temperature are shown in Fig. 3. The FTIR spectrum of precursor is shown in Fig. 3a. The absorption peak corresponding to 3,422 cm^{-1} is related to O–H stretching. The sharp absorption peak corresponding to C–H stretch is observed at 2,982 cm^{-1}. The absorption peak at 2,139 cm^{-1} is due to –C≡C– stretch. The peak at 1,617 cm^{-1} corresponds to the bending mode of H_2O [19]. In addition, a sharp absorption peak prevails around 1,376 cm^{-1} due to C–H rock. The absorption peak at 1,201 and 1,106 cm^{-1} are assigned to C–N stretch. The absorption peak in the lower wave number 567 cm^{-1} is marked by v(M–O) stretch where M = Ti or Cu.

The infrared spectrum of sample calcined at 450 °C is shown in Fig. 3b. The peak at the wave number 3,421 cm^{-1} is due to O–H stretch, 2,923 and 2,368 cm^{-1} are due to C–H stretch, 1,397 cm^{-1} is due to C–H rock, 1,160, 1,113 and 1,020 cm^{-1} are assigned to C–N stretch,

853 cm^{-1} due to =C–H bend mode, and 569 cm^{-1} is assigned to by v(M–O) stretch (where M = Ti or Cu) [22].

The IR spectrum for sample calcined at 550°C (Fig. 3c), shows a reduction in absorption peak intensity at 3,398 cm^{-1}, confirming the prevalence of O–H stretch medium at this stage. The absorption peaks corresponding to 2,344 and 2,364 cm^{-1} are related to very strong C–H stretching. The medium C–H bend mode is present at 1,421 cm^{-1}.

The phase formation of CCTO were further confirmed by FTIR, calcined powder at 850 and 950 °C are shown in Fig. 3d and e. The absorption peak at the wave number 463 cm^{-1} is due to v Ti–O–Ti vibrational mode [20]. The Cu–O bending is observed at 525 cm^{-1}. The Ca–O was observed at 606 cm^{-1} [21]. There are absorption bands in the region 380–700 cm^{-1} arising from the mixed vibrations of CuO_4 and TiO_6 groups prevailing in the CCTO structure [22].

In $CaCu_3Ti_4O_{12}$, Ca^{2+} is dodecahedrally coordinated by oxygen ions, while Cu^{2+} is in square-planar coordination (oxygen as the nearest neighbor) and Ti^{4+} coordinates six oxygen ions in a slightly distorted octahedron (Fig. 4). The TiO_6 groups are tilted by about 20° with respect to the unit cell axis [22]. The crystal structure of $CaCu_3Ti_4O_{12}$ was further refined and found to remain centro symmetric bcc over a wide range of temperatures.

Fig. 3 FT-IR spectra of CCTO (*a*) as precursor, calcined for 3 h in air at (*b*) 450 °C, (*c*) 550 °C, (*d*) 850 °C, and (*e*) 950 °C, respectively
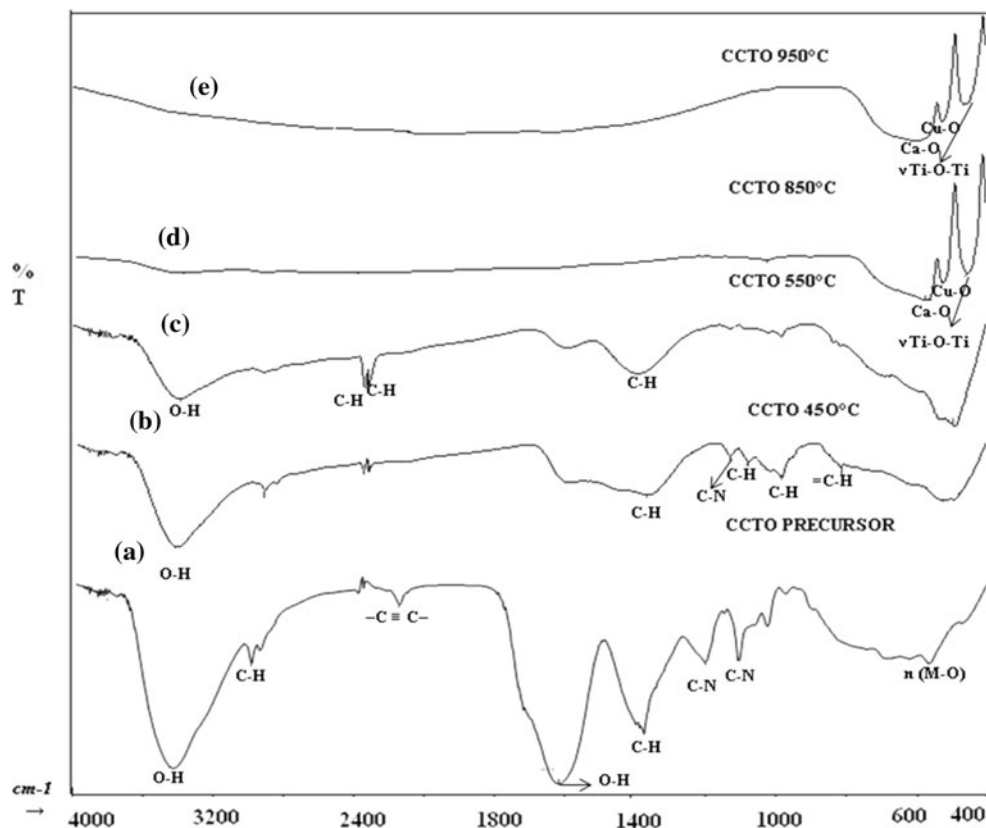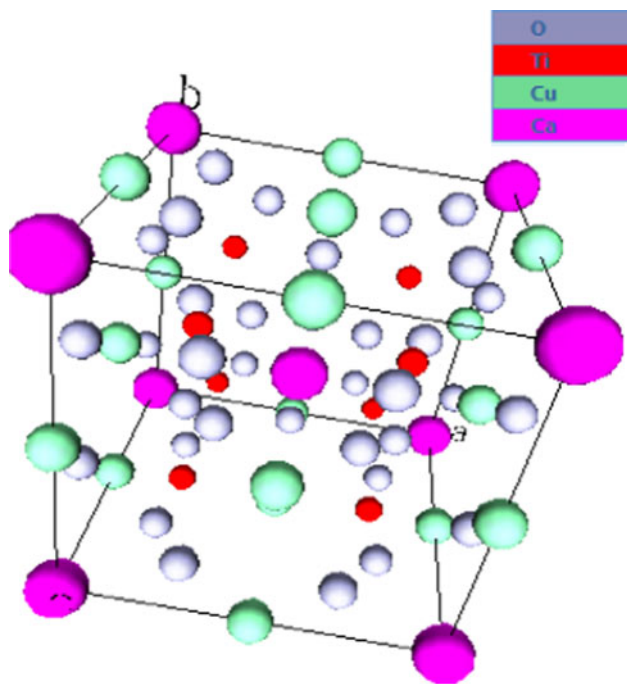
Fig. 4 Structure of $CaCu_3Ti_4O_{12}$ shown as TiO_6 octahedra, Cu atoms bonded to four oxygen atoms, and large Ca atoms without bonds in the cubic cell
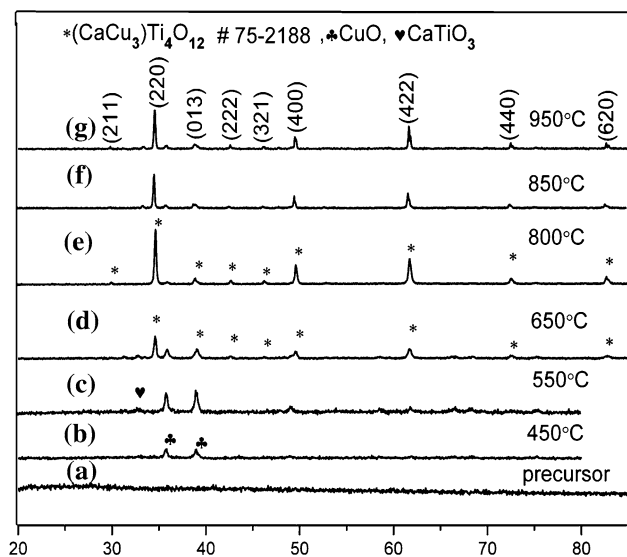

Fig. 5 X-ray diffraction patterns of CCTO (*a*) as precursor, (*b*) heating at 450 °C, (*c*) heating at 550 °C, (*d*) heat treated at 650 °C, (*e*) heat treated at 800 °C, (*f*) heat treated at 850 °C (phase-pure CCTO) and (*g*) heat treated at 950 °C

Figure 5 shows the XRD patterns of the CCTO powder calcined at different temperatures as represented in the figure. The precursor powder is amorphous. The powder calcined at 450 °C shows the peaks corresponding to the formation of CuO. This indicates that, at this stage a minor

crystalline phase of CuO is formed due to thermal decomposition. When the precursor powder is calcined at 550 °C Fig. 5c shows the presence of CuO and $CaTiO_3$ has been observed. The formation of CCTO starts when the precursor is calcined at 650 °C (Fig. 5d), and small amount of $CaTiO_3$ and CuO are also present at this stage [23]. It is confirmed from XRD that the calcium copper titanate (CCTO) is formed when the precursor is heat treated at 800 °C (Fig. 5e). With the increase in the calcination temperature from 650 to 800 °C, the peak corresponding to CCTO increase in intensity and the peaks corresponding to CuO and $CaTiO_3$ decrease and vanish completely, when the calcination temperature at 800 °C. Thus, it is obvious that the single phase CCTO with perovskite structure is formed at 800 °C, which was in good conformity with thermal analysis data. The main peaks of calcined CCTO powders at 800, 850 and 950 °C are compared with the standard powder diffraction pattern (JCPDS card No: 75-2188). The crystallite sizes of the calcined powder at 800 °C is estimated as ~65–75 nm from the X-ray peak broadening using Scherer's formula [23].

$$D = K\lambda/(\beta \cos \theta) \qquad (1)$$

where K is a constant taken as 0.9, θ is the diffraction angle; λ is the wavelength of the X-ray radiation. β is the full width at half maximum (FWHM) of each phase and θ is the diffraction angle.

The major planes corresponding to (211), (220), (013), (222), (321), (400), (422), (440), and (620) are found to be matched which confirmed the presence of Cubic $(CaCu_3)Ti_4O_{12}$ calcined powders. The XRD results of CCTO precursor powder calcined at 800 °C. In addition, no other phases are found in the powder, and the reaction temperature is much lower than that of the solid-state method [1]. The literature survey indicates that the formation temperature of CCTO prepared by solid-state reaction varies from 1,000 to 1,100 °C. It is also interesting to note that the solid-state reaction yields other phases CuO, $CaTiO_3$, TiO_2 phases in addition to CCTO [1, 7]. The lattice constant of CCTO is 7.40 Å, which is in good agreement with the literature value.

The crystalline powder was dispersed in acetone and coated on silicon plate. The coated particles were analyzed by AFM. Figure 6 shows the AFM image of CCTO calcined at 800 °C. The particles shape were spherical and measurement of particle size was 70–80 nm range and of uniform size. This is in good agreement with the X-ray particle size measurement.

The FE-SEM micrographs clearly indicates bi-modal distribution of grains (Fig. 7); the smaller grains have size range from 500 nm to 2 μm and the larger grains have size range from 2 to 6 μm. The bimodal distribution of grains indicates that the sol–gel derived CCTO powders have hard agglomerates which on sintering forms large grains. The
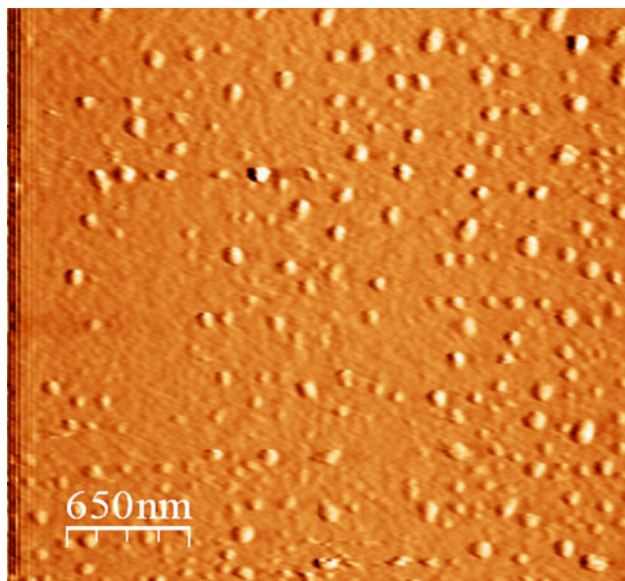
Fig. 6 AFM image of calcined powder at 800 °C in 3 h

Fig. 8 EDX spectra of grains CaCu$_3$Ti$_4$O$_{12}$

1,020 °C (7a) and 1,040 °C (7b) sintered samples show fairly well defined grain sizes with clear grain boundaries. The densest microstructure was obtained for the sample sintered at 1,040 °C for 4 h. The grain size is in the range of 500 nm to 6 μm. The representative EDX spectra for the CCTO are shown in Fig. 8. This clearly shows the presence of Ca, Cu, Ti and O as per stoichiometric ratio in CCTO ceramics, which confirm the purity of the materials.

Figure 9 shows the variation of dielectric constant (Fig. 9a) and loss tangent (Fig. 9b) versus natural log frequency (ln frequency) of CCTO sintered at 1,020 and 1,040 °C at room temperature. The present study reveals that the samples sintered at 1,040 °C/4 h have higher dense microstructure than that sintered at 1,020 °C/4 h. The dielectric constant of CCTO measured at the frequency of 1 kHz, were 2,650 and 23,000, for samples sintered at 1,020 and 1,040 °C. The dielectric constant for the samples
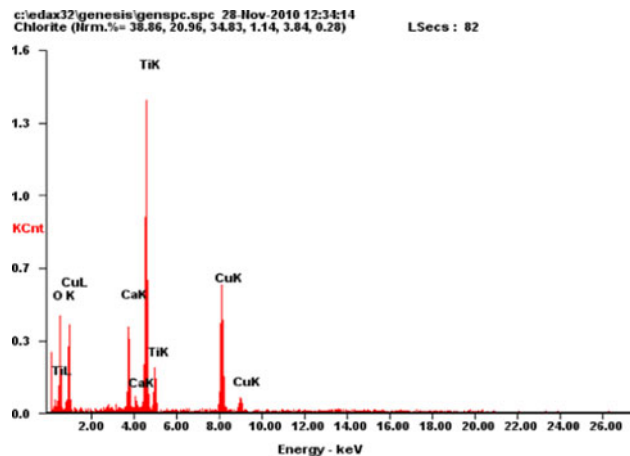
sintered at 1,040 °C, is roughly 10 times higher than that of samples sintered at 1,020 °C. The grain size of the samples sintered at 1,040 °C/4 h also bigger than that sintered at 1,020 °C for 4 h. The dielectric constant of the samples sintered at 1,040 °C for 4 h is very sensitive to frequency. The dielectric constant drops from 50,000 at frequency 50 Hz to 11,000 at frequency 10^6 Hz. The high dielectric constant at low frequency region suggests the possibility that the charge carriers accumulate at the interface of semiconducting grains and insulating grain boundary, which results in interfacial space charge polarization [24]. Li et al. [25] reported that the dielectric constant of polycrystalline CCTO at the high-frequency limit corresponds to that of grain volume, and at the low frequency limit is an apparent value which is the product of the dielectric constant of the grain boundary and the ratio of dimension of the grain to that of the grain boundary. The ''giant'' dielectric constant value for ceramics with higher soaking time and temperature are, therefore, associated with the presence of either thin, reoxidized insulating grain boundary regions and large semiconducting grains or to a
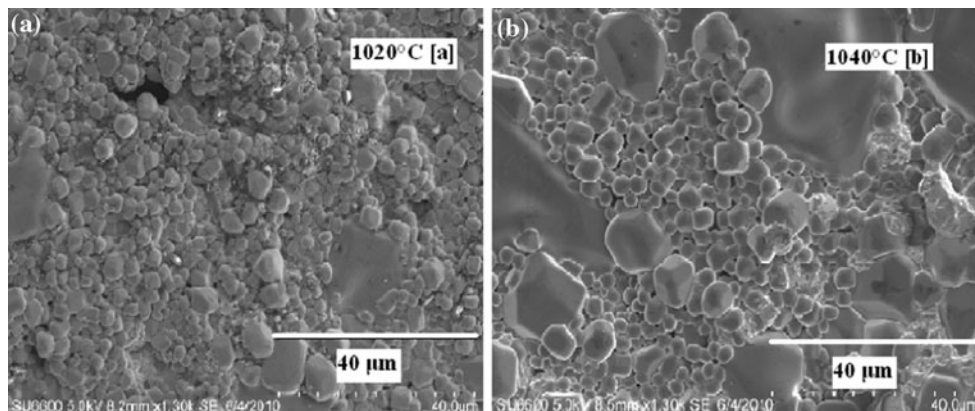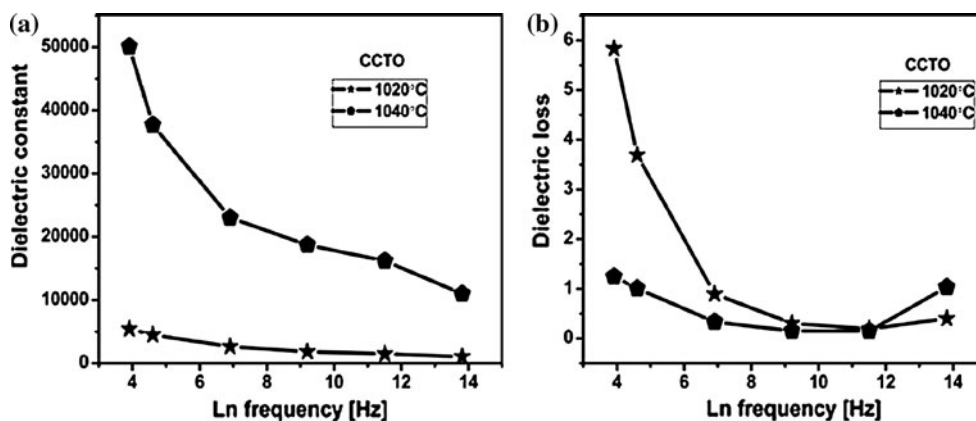

Fig. 7 FESEM micrographs of CCTO ceramics sintered **a** at 1,020 °C for 4 h and **b** at 1,040 °C for 4 h

Fig. 9 Room temperature dielectric constant (**a**) and dielectric loss (**b**) of $CaCu_3Ti_4O_{12}$ sintered at 1,020 and 1,040 °C

secondary phase at the grain boundaries [26], which has not been detected by FE-SEM. $CaCu_3Ti_4O_{12}$. The grain and grain boundary microstructure greatly enhances the dielectric constant [1]. Further work is needed to distinguish these possibilities. The semi conductivity nature of the grains may arise from a small amount of oxygen loss during ceramic processing in air at elevated temperatures, as is known to occur in other titanate-based materials [27]. Specifically, the frequency dependent dielectric behavior has a Debey-like relaxation with a steep decrease in dielectric constant at the frequency where it displays a relaxation peak. The Debye-like relaxation can be explained by the Maxwell–Wagner relaxation at the interfaces between the grains and their boundaries [28–30]. However, in the present study the same could not be observed in the studied frequency range.

The dielectric loss varies from 0.1 to 5.0 for sample sintered at 1,020 °C, and from 0.1 to 1.0 for samples sintered at 1,040 °C. The values of dielectric loss of the samples sintered at 1,040 °C for 4 h are roughly four times lesser than that of the samples sintered at 1,020 °C. The high dielectric constant and low loss are obtained for samples sintered at 1,040 °C for 4 h in the higher frequency region. The high dielectric constant and loss value obtained in this study and measured at room temperature with frequency 50 and 100 Hz. Subramanian et al. [1] first reported that the dielectric constant for CCTO at 1 kHz was around 10,000–12,000. The value of dielectric constant obtained in the present investigation was two times higher than that of the earlier reported values [7]. Generally, CCTO is usually made by traditional solid-state reactions from the metal oxides at high temperatures. This method needs tedious work, relatively long reaction time, and high calcined temperatures. In addition, some secondary phases may appear in ceramics. In contrast, synthesis from a solution affords intimate and homogeneous mixing of the metal ions at the atomic scale, thus reducing the diffusion path length as required. Shorter diffusion length leads to shorter reaction time and lower temperatures [12, 31]. Electrical properties can be considerably improved when the ceramic has homogeneous microstructure. Compared with the traditional mechanical milling method for the preparation of raw powders, the sol–gel one extends the method because it enables the obtained raw ultra-powders to be homogenous in the scale of nano-meter, inducing a fine microstructure of the sintered ceramics [32, 33]. Therefore the product prepared by sol–gel method gives the high dielectric constant compared to other method of preparations. At frequency 1 MHZ the dielectric loss were increased. When the sintering time is increased more oxygen vacancies and space charges are produced and hence dielectric relaxation can be observed giving rise to more dielectric losses [34].

4 Conclusion

Nano powder of calcium copper titanate was successfully synthesized by sol–gel technique. The functional groups were analyzed by using FTIR spectra. The phase formation was confirmed by XRD pattern. The grain size varies from 500 nm to 6 μm as measured by FE-SEM. The CCTO pellet sintered at 1,040 °C exhibits giant dielectric constant value in the order of 10^4 and in particular it was measured about 50,100 at room temperature for 50 Hz. The results indicate the CCTO is a future material in microelectronic industry for various applications.

References

1. M.A. Subramanian, D. Li, N. Duan, B.A. Reisner, A.W. Sleight, J. Solid State Chem. **151**, 323 (2000)
2. A.P. Ramirez, M.A. Subramanian, M. Gardel, G. Blumberg, D. Li, T. Vogt, S.M. Shapiro, Solid State Commun. **115**, 217 (2000)

3. A. Deschanvres, B. Raveau, F. Tollemer, Bull. Chim. Soc. Fr. **11**, 4077 (1967)
4. B. Bochu, M.N. Deschizeaux, J.C. Joubert, A. Collomb, J. Chenavas, M. Marezio, J. Solid State Chem. **29**, 291 (1979)
5. A.M. Glazer, Acta Crystallogr. B **28**, 3384 (1972)
6. R.J. Cava, J. Mater. Chem. **11**, 54 (2001)
7. J.J. Mohamed, S.D. Hutagalung, M.F. Ain, K. Deraman, Z.A. Ahmad, Mater. Lett. **61**, 1835 (2007)
8. S.F. Shao, J.L. Zhang, P. Zheng, C.L. Wang, Solid State Commun. **142**, 281 (2007)
9. S. Kwona, C. Huanga, M.A. Subramanian, D.P. Canna, J. Alloys Compd. **473**, 433 (2009)
10. C.-M. Wanga, K.-S. Kaob, S.-Y. Linc, Y.-C. Chenc, S.-C. Wenga, J. Phys. Chem. Solids **69**, 608 (2008)
11. P. Jha, P. Arora, A.K. Ganguli, Mater. Lett. **4179**, 1 (2002)
12. L. Liu, H. Fan, P. Fang, X. Chen, Mater. Res. Bull. **43**, 1800 (2008)
13. W. Feng, L. Mu-sen, L. Yu-peng, Q. Yong-xin, Mater. Lett. **59**, 916 (2005)
14. A. Hassini, M. Gervais, J. Coulon, V.T. Phoue, F. Gervais, Mater. Sci. Eng. **B87**, 164 (2001)
15. C. Masingboon, P. Thongbai, S. Maensiri, T. Yamwong, S. Seraphin, Mater. Chem. Phys. **109**, 262 (2008)
16. I.V. Morozov, K.O. Znamenkov, Y.M. Korenev, O.A. Shlyakhtin, Thermochim. Acta **403**, 173 (2003)
17. W. Brockner, C. Ehrhardt, M. Gjikaj, Thermochim. Acta **456**, 64 (2007)
18. J. Madarasz, A. Braileanu, G. Pokol, J. Anal. Appl. Pyrolysis **82**, 292 (2008)
19. P. Thomas, K. Dwarakanath, K.B.R. Varma, T.R.N. Kutty, J. Therm. Anal. Calorim. **95**, 267 (2009)
20. A.F.L. Almeida, R.S. de Oliveira, J.C. Goes, J.M. Sasaki, A.G. Souza Filho, J. Mendes Filho, A.S.B. Sombra, Mater. Sci. Eng. **B96**, 275 (2002)
21. X. Sahaya Shajan, C. Mahadevan, Cryst. Res. Technol. **40**, 598 (2005)
22. P. Thomas, K. Dwarakanath, K.B.R. Varma, T.R.N. Kutty, J. Phys. Chem. Solids **69**, 2594 (2008)
23. S. Guillemet-Fritsch, T. Lebey, M. Boulos, B. Durand, J. Eur. Ceram. Soc. **26**, 1245 (2006)
24. H. Birey, J. Appl. Phys. **49**, 2898 (1978)
25. J. Li, K. Cho, N. Wu, A. Ignatiev, IEEE Trans. Dielectr. Electr. Insul. **11**, 534 (2004)
26. T.B. Adams, D.C. Sinclair, A.R. West, Adv. Mater. (Weinheim, Ger.) **18**, 1321 (2002)
27. F.D. Morrison, D.C. Sinclair, A.R. West, J. Am. Ceram. Soc. **84**, 474 (2001)
28. M.H. Cohen, J.B. Neaton, L. He, D. Vanderbilt, J. Appl. Phys. **94**, 3299 (2003)
29. I.P. Raevski, S.A. Prosandeev, A.S. Bogatin, M.A. Malitskaya, L. Jastrabik, J. Appl. Phys. **93**, 4130 (2003)
30. D.P. Cann, S. Aygun, X. Tan, Extended abstracts of the 11th US Japan seminar on dielectric and piezoelectric ceramics, Sapporo, Japan, 2003, pp. 153–156
31. J. Liu, Y. Sui, C. Duan, W. Mei, R.W. Smith, J.R. Hardy, Chem. Mater. **18**, 3878 (2006)
32. S. Jin, H. Xia, Y. Zhang, J. Guo, J. Xu, Mater. Lett. **61**, 1404 (2007)
33. W. Feng, L. Mu-sen, L. Yu-peng, Q. Yong-xin, Mater. Lett. **59**, 916 (2005)
34. B.A. Bender, M.J. Pan, Mater. Sci. Eng. B **117**, 339 (2005)